Photon scanning tunneling microscopy of tailor-made photonic structures

C. Peeters, E. Flück,[a] A. M. Otter, M. L. M. Balistreri, J. P. Korterik, L. Kuipers, and N. F. van Hulst
Applied Optics Group, Faculty of Applied Physics and MESA+ Research Institute, University of Twente, P.O. Box 217, 7500 AE Enschede, The Netherlands

(Received 2 March 2000; accepted for publication 8 May 2000)

Optical field distributions around individually fabricated subwavelength scatterers mapped with a photon scanning tunneling microscope are presented. The photonic structures are produced from ridge waveguides using focused-ion-beam milling. This flexible technique allows us to make single holes and slits of sizes down to 30 nm. A quantitative analysis of the observed optical pattern due to interference between incoming and reflected light yields insight about subwavelength scatterers in waveguides. We conclude that light scattering into high-loss modes of the waveguide occurs. © *2000 American Institute of Physics.* [S0003-6951(00)01327-9]

The continuing miniaturization of optical components such as routers, lasers, filters[1] or switches[2] imposes two demands on research in the field of lightwave devices. First, photonic structures with details on a subwavelength scale are required. Thus, fabrication techniques working beyond the diffraction limit of light are needed. Second, the investigations, necessary to characterize and understand these structures, require an ever-increasing accuracy. Since subtle manipulation of interference effects plays an increasing role in the functionality of lightwave devices, small variations in geometry can have large effects on the light propagation. It is, therefore, desirable to complement conventional input/output experiments with investigation methods that map the optical field distributions inside the structure.

Photon scanning tunneling microscopy (PSTM) is a powerful technique to investigate the optical field distributions in photonic structures.[3–9] This nondestructive technique allows optical details with a resolution beyond the diffraction limit to be determined. In addition, the topography of the photonic structure is measured simultaneously with the optical information. So far, structures that have been investigated with PSTM include waveguides,[4] junctions,[5] and microcavities.[6] PSTM has also been performed on smaller structures, where the optical intensity was measured around particles that had been deposited on a glass surface.[7,8] Recently, direct imaging using a near-field optical microscope of the spatial modes inside a one-dimensional photonic crystal has been reported.[9]

These days, many planar subwavelength structures are fabricated with electron-beam lithography (see, for example, Refs. 10–13). This powerful technique requires highly skilled operators and several fabrication steps. An alternative technique is focused-ion-beam (FIB) milling. With FIB milling, no resist is required and a proficient operator can directly fabricate structures with a high degree of flexibility.

Here, we present subwavelength photonic structures like holes and slits in waveguides fabricated by FIB milling. PSTM measurements of the light fields around these scatterers have been performed with an optical resolution of 50 nm. A quantitative analysis of the observed interference pattern indicates a significant scattering into so-called ''leaky modes.''

The operating principle of a photon scanning tunneling microscope, which is a specific type of near-field scanning optical microscope, is based on the frustration of the evanescent fields above an optical structure. For this, a tapered and coated fiber probe with a subwavelength aperture[14] is approached to within ~20 nm. The evanescent light above the waveguide structure is converted into a propagating wave of the optical fiber and is subsequently detected by a photomultiplier tube. In order to image the optical field distributions of a sample, the fiber probe is kept at a constant distance above the surface by a shear-force feedback system.[15–18] Thus, the topographical image of a structure is obtained by recording the applied voltage of the height piezo. The lateral topographical resolution is of the order of the diameter of the probe end face, whereas the optical resolution is determined by the aperture size of the probe. The aluminum coating of the fiber probes reduces in-coupling of scattered, nonevanescent light, originating from the structure under investigation, into the sides of the probe. The importance of the coating layer for the investigation of strongly scattering structures has recently been confirmed by computer calculations.[19]

The basis for all our structures is a Si_3N_4 ridge waveguide. On top of a 3 μm SiO_2 layer, 55 nm Si_3N_4 is deposited by low-pressure chemical-vapor deposition. Subsequently, a waveguide ridge of 22 nm height and 1.4 μm width is etched by reactive ion etching. Its dimensions are chosen such that only the fundamental waveguide mode (TE_{00}) is supported for light of $\lambda_{HeNe,\,vacuum}=632.8$ nm. The effective index of refraction of this mode is $n_{eff}=1.4636$, as calculated by the effective-index method.[20]

With a FIB machine (FIB 200, FEI), we have succeeded to fabricate nanometer-size structures in the waveguides. 30 keV Ga^+ ions are used to sputter material from the sample, resulting in holes and/or slits. The focal spot size and the applied current, which can be varied in discreet steps between 1 and 70 pA, determine the beam density [A/m^2]. The fabricated structures include holes with diameters of 30–250

[a]Author to whom correspondence should be addressed; electronic mail: e.flueck@tn.utwente.nl

 © 2000 American Institute of Physics
Downloaded 01 Sep 2003 to 130.89.25.109. Redistribution subject to AIP license or copyright, see http://ojps.aip.org/aplo/aplcr.jsp

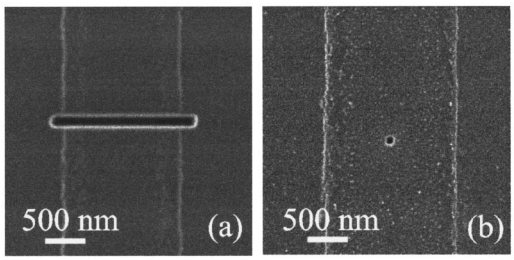

FIG. 1. Focused-ion-beam images of Si_3N_4 ridge waveguides (top view), containing subwavelength scatterers. (a) Waveguide with a focused-ion-beam-milled slit of 1.8 μm×160 nm. (b) Waveguide with a focused-ion-beam-milled hole with a diameter of 80 nm.

nm and slits of widths and length of 80–100 nm and 1.8 μm, respectively. It turns out that the minimal size of the fabricated features is not solely determined by the minimal focal spot size (~10 nm) of the FIB, but also by the exposure time. Increasing the milling time results in larger hole diameters. We attribute this effect to a charging of the nonconducting Si_3N_4. The depth of the holes and slits is not exactly known, but certainly deeper than the Si_3N_4 layer. Figure 1 shows two examples of subwavelength structures produced with the FIB. The two images were acquired by scanning the ion beam over the surface with an ion current of 12 pA and collecting secondary electrons coming from the sample. For the fabrication of the slit [Fig. 1(a)], a beam current of 4 pA and an exposure time of 57 s were used. The hole [Fig. 1(b)] was produced with an exposure time of 5 s. Note that care needs to be taken while imaging with the FIB in order to prevent unwanted damage to the sample.

PSTM measurements of a waveguide containing a single slit are shown in Fig. 2. In the topographical image [Fig. 2(a)], both the ridge waveguide and the slit are clearly visible. The measurements show a height resolution of 0.5 nm and a lateral topographical resolution better than 50 nm. The optical image [Fig. 2(b)] shows an interference pattern, consisting of high- and low-intensity stripes perpendicular to the propagation direction of guided light in the waveguide. In effect, it is a standing wave resulting from the interference between incoming (from top to bottom in the image) and backscattered light. Just in front of the slit itself, an increased intensity is observed. We attribute the first intense ''fringe'' to light that is scattered directly into the probe aperture by the slit. Measurements with uncoated fiber probes contained

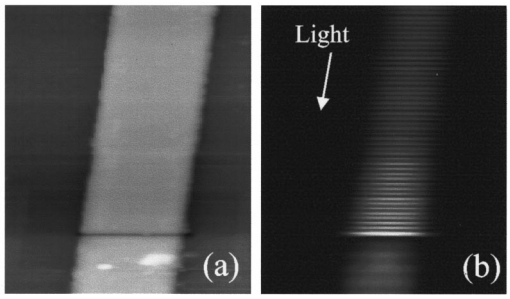

FIG. 2. Topography (a) and optical (b) images of a waveguide with one slit, simultaneously obtained with photon scanning tunneling microscopy. Image size: 13 μm (vertical)×4.0 μm (horizontal). (a) Topography of the modified ridge waveguide. Lateral resolution: ~50 nm. (b) Optical field distribution in the waveguide. Incoming light (arrow indicates direction) interferes with light reflected at the slit producing the striped standing-wave pattern.

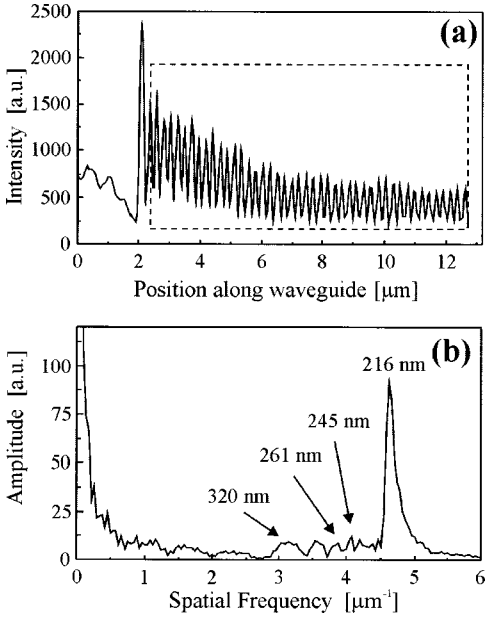

FIG. 3. (a) Intensity graph constructed by summing up 80 line traces of the optical image along the waveguide. (b) Fourier transform of boxed area of (a). The clear peak corresponding to a periodicity of 216 nm indicates that the interference pattern is dominated by a standing wave set up by an incoming and a reflected TE_{00} mode. The peaks at lower spatial frequencies (indicated by the arrows) are the result of interference between the TE_{00} mode and ''leaky modes.''

so much of this stray light that investigations in a region of 680 nm around the slit were impossible. Further, Fig. 2(b) shows that some light is transmitted through the slit and reappears as a guided mode in the waveguide after the slit.

The graph shown in Fig. 3(a) is generated by summing up 80 line traces of the optical image (line traces are taken parallel along the waveguide). The averaged intensity decay of light before the slit excluding the first maximum in Fig. 3(a) can be fitted with an exponential decay of $e^{-\beta x}$, with $\beta=10\ \mu m^{-1}$. The modulation depth M of the interference pattern is given by $M=(I_{max}-I_{min})/(I_{max}+I_{min})$. For positions more than 3 μm in front of the slit, the modulation depth is found to be 0.7. This would correspond to an amplitude reflection coefficient of 41%. However, closer to the slit, the modulation depth is less (0.45 at 2 μm from the slit). The decrease in modulation depth closer to the slits indicates a reduced degree of coherence compared to the coherence found further from the slit.

A Fourier transformation [Fig. 3(b)] of a range of 10.5 μm of the intensity graph in Fig. 3(a) (boxed area) shows a strong peak corresponding to a periodicity of 216 (±2) nm. The observed periodicity of 216 nm corresponds well to half of the calculated wavelength of the TE_{00} mode (216.2 nm) in our Si_3N_4 structure, because light of $\lambda_{HeNe,\ vacuum}=632.8$ nm has a wavelength of 432.4 nm ($n_{eff}=1.4636$). This indicates that the observed interference pattern is indeed dominated by a standing wave set up by reflected and unreflected TE_{00} modes. However, at lower spatial frequencies additional peaks are visible, as indicated by arrows in Fig. 3(b).

We attribute the reduced modulation depth closer to the slit, the exponential decay of the average intensity, and the peaks at lower spatial frequencies to the existence of so-called ''leaky modes'' propagating in the direction opposite to the incoming light. These ''leaky modes'' have different

Downloaded 01 Sep 2003 to 130.89.25.109. Redistribution subject to AIP license or copyright, see http://ojps.aip.org/aplo/aplcr.jsp

wavelengths than the TE_{00} mode and are not supported by the waveguide itself. They, therefore, have a high loss rate, which would explain the exponential intensity decay. Their different wavelengths also lead to the decreased coherence (lower modulation depth) observed close to the slit. To verify the existence of ''leaky modes,'' we have calculated the interference length between the theoretically calculated ''leaky modes'' with the incoming fundamental TE_{00} mode of the waveguide. The arrows in Fig. 3(b) indicate three theoretically calculated interference lengths. The height of the indicated peaks decreases with increasing distance from the slits. This confirms the high-loss rates associated with the ''leaky modes.'' Thus, apparently the scattering of light, probably due to roughness or the edges of the slit walls, excites these modes. In all probability, the low spatial frequency peaks also contain a contribution due to interference of light above the waveguide with light inside the waveguide. The observation of light scattering into ''leaky modes'' exemplifies the power of PSTM to identify local properties of optical fields inside a structure, which would not be observed by conventional input/output measurements.

PSTM is presented as a powerful technique for characterizing photonic structures. PSTM measurements on optical waveguides containing subwavelength scatterers like holes and slits are shown. Simultaneous with the topography, the optical field distributions are mapped with a resolution of 50 nm. We showed that by focused-ion-beam milling nanometer-scale details could be successfully fabricated. A quantitative analysis of the interference pattern around subwavelength scatterers indicates—in addition to the expected standing-wave pattern—scattering into ''leaky modes.''

This work is part of the research program of the ''Stichting for Fundamenteel Onderzoek der Materie (FOM),'' which is financially supported by the ''Nederlandse Organisatie voor Wetenschappelijk Onderzoek (NWO).'' C. van Os is gratefully acknowledged for the fabrication of the waveguides.

[1] B. J. Offrein, G. L. Bona, F. Horst, H. W. M. Salemink, R. Beyeler, and R. Germann, IEEE Photonics Technol. Lett. **11**, 239 (1999).
[2] E. Flück, F. Horst, B. J. Offrein, R. Germann, H. W. M. Salemink, and G. L. Bona, IEEE Photonics Technol. Lett. **11**, 1399 (1999).
[3] P. L. Phillips, J. C. Knight, B. J. Mangan, and P. St. J. Russell, M. D. B. Charlton, and G. J. Parker, J. Appl. Phys. **85**, 6337 (1999).
[4] A. G. Choo, M. H. Chudgar, H. E. Jackson, G. N. DeBrabander, M. Kumar, and J. T. Boyd, Ultramicroscopy **57**, 124 (1995).
[5] H. E. Jackson, S. M. Lindsay, C. D. Poweleit, D. H. Naghski, G. N. DeBrabander, and J. T. Boyd, Ultramicroscopy **61**, 295 (1995).
[6] M. L. M. Balistreri, D. J. W. Klunder, J. P. Korterik, F. C. Blom, A. Driessen, H. W. J. M. Hoekstra, L. Kuipers, and N. F. van Hulst, Opt. Lett. **24**, 1829 (1999).
[7] N. F. van Hulst, F. B. Segerink, F. Achten, and B. Bölger, Ultramicroscopy **42-44**, 416 (1991).
[8] J. R. Krenn, A. Dereux, J. C. Weeber, E. Bourillot, Y. Lacroute, J. P. Goudonnet, G. Schider, W. Gotschy, A. Leitner, F. R. Aussenegg, and C. Girard, Phys. Rev. Lett. **82**, 2590 (1999).
[9] G. H. Vander Rhodes, M. S. Ünlü, B. B. Goldberg, J. M. Pomeroy, and T. F. Krauss, IEE Proc.-J: Optoelectron. **145**, 379 (1998).
[10] E. Yablonovitch, Phys. Rev. Lett. **58**, 2059 (1987).
[11] J. S. Foresi, P. R. Villeneuve, J. Ferrera, E. R. Thoen, G. Steinmeyer, S. Fan, J. D. Joannopoulos, L. C. Kimerling, H. I. Smith, and E. P. Ippen, Nature (London) **390**, 143 (1997).
[12] C. C. Cheng and A. Scherer, J. Vac. Sci. Technol. B **13**, 2696 (1995).
[13] T. F. Krauss, R. M. De la Rue, and S. Brand, Nature (London) **383**, 699 (1996).
[14] J. A. Veerman, A. M. Otter, L. Kuipers, and N. F. van Hulst, Appl. Phys. Lett. **72**, 3115 (1998).
[15] R. Toledo-Crow, P. C. Yang, Y. Chen, and M. Vaez-Iravani, Appl. Phys. Lett. **60**, 2957 (1992).
[16] E. Betzig, P. L. Finn, and J. S. Weiner, Appl. Phys. Lett. **60**, 2484 (1992).
[17] K. Karrai and R. D. Grober, Appl. Phys. Lett. **66**, 1842 (1995).
[18] A. G. T. Ruiter, J. A. Veerman, K. O. van der Werf, and N. F. van Hulst, Appl. Phys. Lett. **71**, 28 (1997).
[19] S. Fan and J. D. Joannopoulos, Appl. Phys. Lett. **75**, 3461 (1999).
[20] *Integrated Optics*, edited by T. Tamir (Springer, Berlin, 1975).

Downloaded 01 Sep 2003 to 130.89.25.109. Redistribution subject to AIP license or copyright, see http://ojps.aip.org/aplo/aplcr.jsp